DOI: 10.1002/anie.201100432

Endofullerenes

# Covalently Linked Porphyrin–La@$C_{82}$ Hybrids: Structural Elucidation and Investigation of Intramolecular Interactions**

*Lai Feng, Zdenek Slanina, Satoru Sato, Kenji Yoza, Takahiro Tsuchiya, Naomi Mizorogi, Takeshi Akasaka,* Shigeru Nagase,* Nazario Martín, and Dirk M. Guldi*

*Dedicated to Professor Luis Echegoyen on the occasion of his 60th birthday*

The study of covalent and non-covalent photoactive hybrids continues to be of interest for developing photosynthetic and optoelectronic applications.[1] To this end, $C_{60}$ is recognized as an important building block owing to its rich redox properties and low reorganization energy in electron-transfer reactions. Hybrids of $C_{60}$ with various photoactive and electroactive units have been studied comprehensively in the context of light harvesting, unidirectional energy transfer, and electron transfer.[2] Recently, the unique structures and properties of endohedral metallofullerenes (EMFs), such as $M_3N@C_{80}$ (M = Sc, Lu) and $M_2@C_{80}$ (M = La, Ce), has led to their integration into photoactive hybrids in which improved or switchable inter- or intramolecular electron transfer events were realized.[3,4]

Another widely studied EMF is La@$C_{2v}$–$C_{82}$, which features a huge anionic π surface and an open-shell structure. Importantly, in comparison to $C_{60}$ and the above-mentioned EMFs, La@$C_{82}$ has more active redox properties, a broader absorption spectrum, a smaller band gap, and lower-lying excited state.[5,6] In this regard, incorporating La@$C_{82}$ into multichromophoric systems is certainly worthy of consideration. In fact, recent efforts have exemplified the construction of supramolecular arrays of La@$C_{82}$ and chromophores, such as porphyrins.[7] However, covalently linked hybrids remain unexplored. A likely rationale includes the presence of multiple isomeric products that are formed in most reactions.[8] Herein, we present three isomeric covalently linked 5,10,15,20-tetraphenylporphyrin ($H_2$Por)–La@$C_{82}$ hybrids, including their synthesis, electrochemistry, and spectroscopic and computational studies. Compared with non-covalent hybrids,[7b] the presence of a flexible linker between the two subunits is evidently crucial. It facilitates π–π attractions between the two subunits and therefore enhances intramolecular electronic interactions even in the ground state. Remarkable fluorescence quenching in all covalently linked hybrids is evidence of the occurrence of photoinduced intramolecular communication.

The synthesis started with a thermal reaction (Scheme 1) involving La@$C_{82}$ and a typical diazo precursor **1** that was used to synthesize the [6,6]-phenyl-$C_{61}$ butyric acid methyl ester (PCBM).[10] Following a multistage separation using HPLC, three isomeric monoadducts ($M_1$, $M_2$, and $M_3$)[11] were ultimately isolated as major products. Substitution of **1** by another precursor, **2**, led to the synthesis of $H_2$Por–La@$C_{82}$ hybrids. In a similar way, three isomeric forms ($M_1$Por, $M_2$Por, and $M_3$Por) were isolated as major products with lower yields.

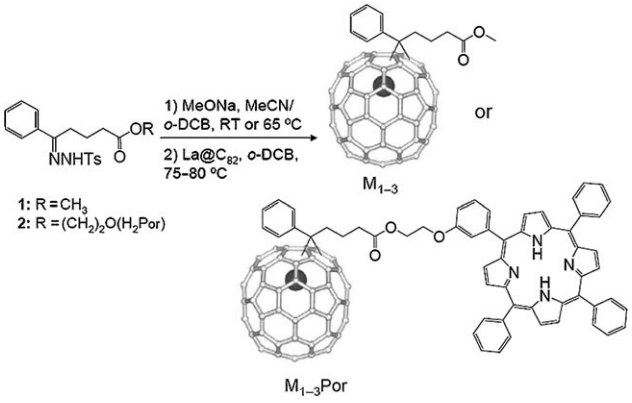


***Scheme 1.*** Synthesis of $M_{1-3}$ and $M_{1-3}$Por. Ts = toluene-4-sulfonyl, *o*-DCB = 1,2-dichlorobenzene.

[*] Dr. L. Feng, Dr. Z. Slanina, Dr. S. Sato, Dr. T. Tsuchiya, Dr. N. Mizorogi, Prof. Dr. T. Akasaka
Centre for Tsukuba Advanced Research Alliance
University of Tsukuba, Ibaraki 305-8577 (Japan)
Fax: (+81) 298-53-6409
E-mail: akasaka@tara.tsukuba.ac.jp
Dr. K. Yoza
Bruker, Kanagawa (Japan)
Prof. Dr. S. Nagase
Department of Theoretical and Computational Molecular Science
Institute for Molecular Science
Okazaki, Aichi 444-8585 (Japan)
E-mail: nagase@ims.ac.jp
Prof. Dr. N. Martín
Departamento de Química Orgánica
Universidad Complutense, Madrid (Spain)
Prof. Dr. D. M. Guldi
Department of Chemistry and Pharmacy & Interdisciplinary Center for Molecular Materials, Universität Erlangen-Nürnberg (Germany)

[**] This work was supported in part by a Grant-in-Aid for Scientific research on Innovative Areas (No. 20108001, "pi-Space"), a Grant-in-Aid for Scientific Research (A) (No. 20245006), The Next Generation Super Computing Project (Nanoscience Project), Nanotechnology Support Project, and Grants-in-Aid for Scientific research on Priority Area (Nos. 20036008, 20038007), and Specially Promoted Research from the Ministry of Education, Culture, Sports, Science, and Technology of Japan. Technology of Japan and The Strategic Japanese–Spanish Cooperative Program is funded by JST and MICINN.

Supporting information for this article is available on the WWW under http://dx.doi.org/10.1002/anie.201100432.

All compounds were characterized using HPLC, MALDI-MS, EPR, and UV/Vis-NIR spectroscopy.[9] The HPLC profiles of all the purified samples are shown in the Supporting Information, Figures S1, S2. The MS spectra (Supporting Information, Figures S3, S4) display a dominant molecular ion peak either at *m*/*z* 1314 for $M_{1-3}$ or at *m*/*z* 1957 for $M_{1-3}$Por. Agreement between the observed and the calculated isotopic distributions confirms their compositions. The absence of other fragment peaks suggests their high stability under the laser decomposition conditions. Unambiguous structural determination was achieved by means of crystallography. As shown in Figure 1, $M_3$ is a [6,6]-open adduct.[12] The C2–C3 bond is cleaved because of the [1+2]-addition, and the La atom is close to the addition site, with 100% occupancy. The addition pattern and the addition site are identical to those proposed for La@$C_{82}$Ad-II (Ad = adamantylidene, minor isomer),[13] probably indicating their similar formation pathway, that is, carbene addition.

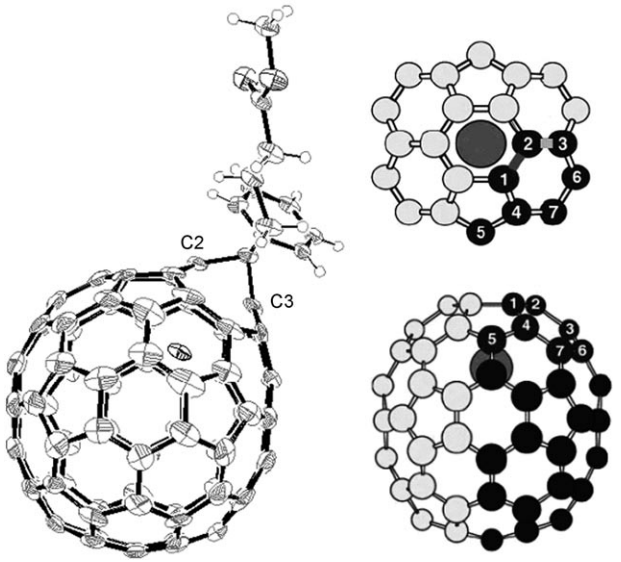


***Figure 1.*** ORTEP of $M_3$ (ellipsoids set at 50% probability) and orthogonal views of the addition site.

The absorption spectra of $M_{1-3}$ and $M_{1-3}$Por are portrayed in Figure 2 (see the Supporting Information, Figure S5 for visible absorptions of $M_{1-3}$). As for $M_3$, the two NIR absorptions at around 986 and 1525 nm are fully consistent with those seen for La@$C_{82}$Ad-II,[13] reflecting their isostructural nature. For $M_1$ and $M_2$, they both show absorptions at 1010 and 1456 nm; the form of these absorptions resemble those of La@$C_{82}$Ad-I (major isomer).[14] Considering that the electronic spectra of La@$C_{82}$ derivatives usually reflect the fingerprints of their π-system topology, it is reasonable to assume the isostructural nature of the respective adducts; that is, the same addition pattern and the same addition site (C1 and C2). Consequently, $M_1$ and $M_2$ might be stereoisomers of the 1,2-adduct that possesses two chiral centers (that is, C1 and the spiro carbon).

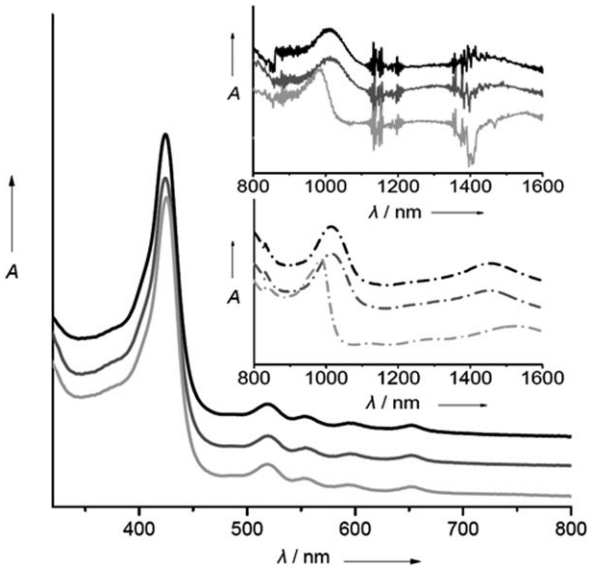


***Figure 2.*** UV/Vis absorption spectra of $M_{1-3}$Por hybrids ($M_1$ black, $M_2$ dark gray, $M_3$ light gray lines) at similar concentrations in toluene. Inset: NIR absorption spectra of $M_{1-3}$Por hybrids (upper, lines) and $M_{1-3}$ references (lower, dashed lines).

Each hybrid ($M_{1-3}$Por) exhibits the same NIR absorption features as their corresponding reference compounds, namely $M_{1-3}$. In the visible range, all of the hybrids reveal $H_2$Por-centered Soret and Q bands at 425 nm and 519, 553, 595, 653 nm, respectively. However, relative to $H_2$Por ($\varepsilon_{418\,nm}$ = 490000 L mol$^{-1}$ cm$^{-1}$), the Soret bands of $M_{1-3}$Por are broadened, with reduced molar absorptivity ($\varepsilon_{425\,nm}$ ≈ 287500 L mol$^{-1}$ cm$^{-1}$), and are red-shifted by 7 nm. Likewise, the Q bands undergo red-shifts that range from 3 to 5 nm. All of these spectral changes suggest appreciable electronic interactions between the two subunits of these covalently linked hybrids in the ground state. As reference, the absorption spectrum (Figure S6)[9] of an equimolar mixture of $H_2$Por and La@$C_{82}$ appears as a simple superimposition of the two species, indicating the lack of interaction between the noncovalently linked $H_2$Por and La@$C_{82}$.

The EPR spectra of all of the compounds are shown in Figure S7, and the corresponding features are summarized in Table S1.[9] All of the three hybrids display distinct octet EPR signals with characteristic *hfcc* and *g*-factor parameters, reflecting their paramagnetic properties. Importantly, the spectral resemblance between the hybrids and the references constitutes additional evidence for their structural similarity.

Electrochemical studies with $M_{1-3}$ and $M_{1-3}$Por were carried out in *o*-dichlorobenzene containing 0.05 M $Bu_4NPF_6$ under an argon atmosphere. The corresponding differential pulse voltammograms (DPVs) are depicted in Figures S8–13,[9] and the potentials versus Fc/Fc$^+$ are summarized in Table 1. Using $H_2$Por and $M_{1-3}$ as references assisted in determining the redox properties of $M_{1-3}$Por. In the anodic direction, $M_{1-3}$Por have four one-electron oxidation steps. The first and fourth steps, between −0.02 and −0.04 V and between 1.06 and 1.13 V, were assigned to La@$C_{82}$ centered processes, while the second and third steps, between 0.57 and

  

***Table 1:*** Redox potentials of $M_{1-3}$Por hybrids, $M_{1-3}$ references, and $H_2$Por.[a]

| | $E_4^{ox}$ | $E_3^{ox}$ | $E_2^{ox}$ | $E_1^{ox}$ | $E_1^{red}$ | $E_2^{red}$ | $E_3^{red}$ | $E_4^{red}$ |
|---|---|---|---|---|---|---|---|---|
| $H_2$Por | | 1.16 | 0.94 | 0.52 | −1.75 | −2.07 | | |
| $M_1$Por | 1.13 | 0.89 | 0.58 | −0.03 | −0.48 | −1.41 | −1.74 | −2.07 |
| $M_2$Por | 1.06 | 0.89 | 0.57 | −0.04 | −0.48 | −1.41 | −1.75 | −2.06 |
| $M_3$Por | 1.08 | 0.89 | 0.61 | −0.02 | −0.45 | −1.36 | −1.71 | −2.07 |
| $M_1$ | | | | 0.02 | −0.42 | −1.37 | −1.71 | |
| $M_2$ | | | 1.18 | 0.02 | −0.43 | −1.38 | −1.71 | |
| $M_3$ | | | | 0.01 | −0.43 | −1.38 | −1.74 | |

[a] Values given versus $Fc^+/Fc$. DPV measurements in *o*-DCB solution using 0.05 M $Bu_4NPF_6$ as supporting electrolyte, ferrocene as an internal standard, platinum wires as the working and counter electrodes, and SCE as the reference electrode. Scan rate: 20 mV $s^{-1}$.

0.61 V and at 0.89 V, relate to processes involving $H_2$Por. In the cathodic direction, $M_{1-3}$Por reveal four reduction steps. The first, second, and fourth steps, between −0.45 and −0.48 V, between −1.36 and −1.41 V, and between −2.06 and −2.07 V, correlate to the one-electron reduction of La@$C_{82}$, La@$C_{82}$, and $H_2$Por, respectively. The third step between −1.71 and −1.75 V, which is evidently a two-electron reduction, is expected to involve La@$C_{82}$ and $H_2$Por. Notably, the La@$C_{82}$-centered redox processes, including the first oxidation and first reduction, are cathodically shifted by 30–60 mV and 20–60 mV, respectively, for $M_{1-3}$Por as compared with those noted for $M_{1-3}$. In contrast, the $H_2$Por-centered redox process, that is, the second oxidation of $M_{1-3}$Por, is shifted anodically by 50–90 mV relative to that of $H_2$Por. The aforementioned observations lead us to conclude that sizeable interactions prevail between the two subunits in the ground state.

To gain further insights into the molecular and electronic structure of the hybrids, computational studies were performed using density functional methods (DFT) at the M06-2X/3-21G-LanL2DZ level for geometry optimizations and higher levels (that is, M06/and M06-2X/6-31G*-LanL2DZ)[15] for energy calculations with the Gaussian 09 program.[16] The optimized structure of $M_3$Por with a folded and a stretched conformation is shown in Figure 3. Importantly, the former conformer is 16.3 or 14.5 kcal $mol^{-1}$ more stable than the latter, suggesting sizable intramolecular attractions. In the folded conformer, the neighboring distance between the two subunits is 2.87 Å, which is shorter than the sum of van der Waals radii. As Figures 4 and S14 reveal,[9] the calculated SOMO and LUMO are mainly localized on La@$C_{82}$, while the

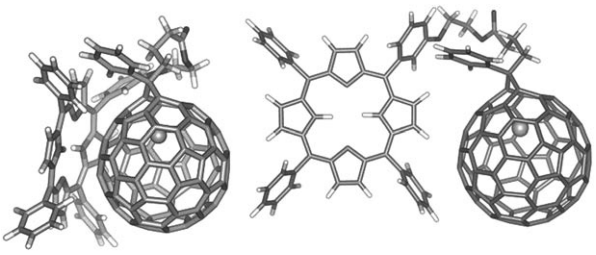

***Figure 3.*** Two optimized conformers of $M_3$Por at the M06-2X/3-21G-LanL2DZ level. The folded conformer (left) is 14.5 kcal $mol^{-1}$ more stable than stretched conformer (right) at this level.

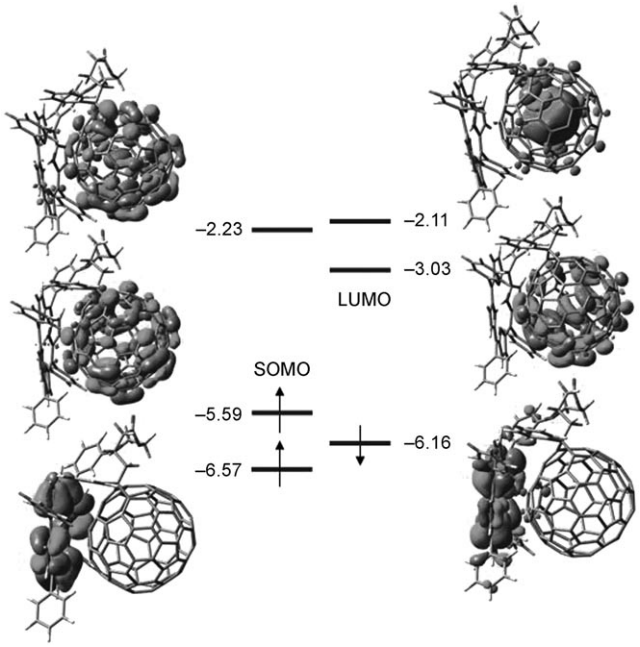


***Figure 4.*** MO diagram of the $M_3$Por hybrid. Values are given in eV.

HOMO is centered on $H_2$Por, in close agreement with the results of electrochemical studies. On the other hand, a delocalization of the SOMO on $H_2$Por and of the β-HOMO on La@$C_{82}$ (< 2%) was observed only for the folded conformer, indicating a distance-dependent interaction between the two components.

Intramolecular interactions in the excited state were probed by means of steady-state fluorescence spectra, which were recorded in an argon-saturated toluene solution. Importantly, as Figures 5 and S15 show, the strong fluorescence of $H_2$Por with a quantum yield of 0.11[17] is subject to a remarkable quenching in $M_{1-3}$Por, with quantum yields of approximately $(2.2 \pm 0.5) \times 10^{-4}$. As a reference experiment, an equimolar mixture of La@$C_{82}$ and $H_2$Por at a similar concentration was tested in which fluorescence quenching was almost negligible (Figure S16).[9] We therefore concluded

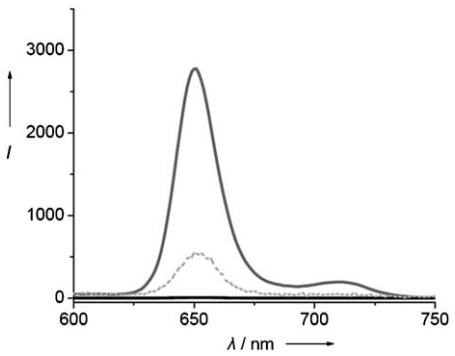


***Figure 5.*** Steady-state fluorescence spectra of $M_3$Por (black line) and $H_2$Por (dark gray line) in toluene solution, photoexcited at 413 nm after normalization to the absorption intensity (0.34) at the excitation wavelength. The fluorescence intensity of $M_3$Por is also shown amplified by a factor of 100 (gray dashed line).

  

that the excited state deactivation might proceed by either an intramolecular energy or electron transfer process. The hypothesis of an energy transduction evolving from photo-excited $H_2$Por to La@$C_{82}$ seems to be more reasonable. In particular, the energy level of the first doublet excited state of La@$C_{82}$ is about 0.88 eV,[6] which is more than 1.0 eV below the first singlet excited state of $H_2$Por (1.90 eV) in toluene.[18] Electron transfer, on the other hand, appears to be thermodynamically less-favored, considering that the energy level of the radical ion pair state, namely $(La@C_{82})^{-}$-$(H_2Por)^{\bullet+}$, is 1.05 eV.[19]

In conclusion, we have presented the synthesis of three isomeric covalently linked porphyrin–La@$C_{82}$ hybrids ($M_{1-3}$Por) and their structural characterization. Combined spectroscopy, electrochemistry, and DFT calculations suggest identifiable electronic interactions between the two subunits in the ground state. In the excited state, nearly quantitative quenching of the $H_2$Por fluorescence suggests that the two chromophores do communicate with each other in the form of an energy/electron transfer event. These covalent hybrids may be useful in future design and creation of EMF-based materials for molecular electronic devices and photovoltaics. More precise characterization of the photophysical properties of these new hybrids will be undertaken in future research.

## Experimental Section

Details of the syntheses are given in the Supporting Information. A black single crystal of $M_3$ was obtained by layering a $CS_2$ solution with hexane. X-ray data were collected with an AXS SMART APEX machine (Bruker Analytik, Germany) at 120 K. CCDC 807837 contains the supplementary crystallographic data for this paper. These data can be obtained free of charge from The Cambridge Crystallographic Data Centre via www.ccdc.cam.ac.uk/data_request/cif.

Calculations were carried out using the hybrid density functional theory (DFT) at the M06 and M06-2X levels with the relativistic effective core potential as implemented in the Gaussian 09 software package.[16] The LANL2DZ basis set was employed for La and 3-21G (geometry optimization) and 6-31G* (energy calculation) basis set for C, H, O, and N.

Received: January 18, 2011
Revised: February 24, 2011
Published online: May 12, 2011

**Keywords:** density functional calculations · fullerenes · lanthanum · π interactions · structure elucidation

[1] For recent reviews, see: a) M. R. Wasielewski, *Acc. Chem. Res.* **2009**, *42*, 1910 – 1921; b) D. Gust, T. A. Moore, A. L. Moore, *Acc. Chem. Res.* **2009**, *42*, 1890 – 1898; c) J. L. Delgado, P.-A. Bouit, S. Filippone, M. Á. Herranz, N. Martín, *Chem. Commun.* **2010**, *46*, 4853 – 4865.

[2] *Fullerenes: From Synthesis to Optoelectronic Properties* (Ed.: D. M. Guldi, N. Martín), Kluwer Academic Publishers, Dordrecht, The Netherlands, **2002**.

[3] a) J. R. Pinzón, M. E. Plonska-Brzezinska, C. M. Cardona, A. J. Athans, S. G. Sankaranarayanan, D. M. Guldi, M. A. Herranz, N. Martin, T. Torres, L. Echegoyen, *Angew. Chem.* **2008**, *120*, 4241 – 4244; *Angew. Chem. Int. Ed.* **2008**, *47*, 4173 – 4176; b) J. R. Pinzón, et al., *Chem. Eur. J.* **2009**, *15*, 864 – 877; c) J. R. Pinzón, D. C. Gasca, S. G. Sankaranarayanan, T. Bottari, D. M. Guldi, L. Echengoyen, *J. Am. Chem. Soc.* **2009**, *131*, 7727 – 7734; d) R. B. Ross, et al., *Nat. Mater.* **2009**, *8*, 208 – 212.

[4] a) Y. Takano, Á. Herranz, N. Martín, S. G. Radhakrishnan, D. M. Guldi, T. Tsuchiya, S. Nagase, T. Akasaka, *J. Am. Chem. Soc.* **2010**, *132*, 8048 – 8055; b) D. M. Guldi, et al., *J. Am. Chem. Soc.* **2010**, *132*, 9078 – 9086.

[5] T. Akasaka, S. Nagase, *Endofullerenes: A New Family of Carbon Clusters*, Kluwer, Dordrecht, **2002**.

[6] a) M. Fujitsuka, O. Ito, K. Kobayashi, S. Nagase, K. Yamamoto, T. Kato, T. Wakahara, T. Akasaka, *Chem. Lett.* **2000**, 902 – 903; b) K. Yanagi, S. Okubo, T. Okazaki, H. Kataura, *Chem. Phys. Lett.* **2007**, *435*, 306 – 310.

[7] a) G. Gil-Ramírez, S. D. Karlen, A. Shundo, K. Porfyrakis, Y. Ito, G. A. D. Briggs, J. J. L. Morton, H. L. Anderson, *Org. Lett.* **2010**, *12*, 3544 – 3547; b) G. Pagona, S. P. Economopoulos, T. Aono, Y. Miyata, H. Shinohara, N. Tagmatarchis, *Tetrahedron Lett.* **2010**, *51*, 5896 – 5899.

[8] a) B. Cao, T. Wakahara, Y. Maeda, A. Han, T. Akasaka, T. Kato, K. Kobayashi, S. Nagase, *Chem. Eur. J.* **2004**, *10*, 716 – 720; b) M. Yamada, et al., *J. Phys. Chem. B* **2005**, *109*, 6049 – 6051; c) L. Feng, et al., *Chem. Eur. J.* **2006**, *12*, 5578 – 5586; d) Y. Takano, et al., *J. Am. Chem. Soc.* **2008**, *130*, 16224 – 16230.

[9] See the Supporting Information.

[10] J. C. Hummelen, B. W. Knight, F. LePeq, F. Wudl, J. Yao, C. L. Wilkins, *J. Org. Chem.* **1995**, *60*, 532 – 538.

[11] The arabic numbers (i.e., 1, 2, 3) refer to the isomeric monoadducts of La@$C_{82}$ in terms of increasing retention time on the HPLC.

[12] Crystal data for $(\mathbf{M_3})\cdot 2CS_2$: $C_{96}H_{14}LaO_2S_4$, $M_r = 1466.22$, black chip, $0.39 \times 0.28 \times 0.06$ mm$^3$, monoclinic, space group $P2_1/c$, $a = 14.587(2)$ Å, $b = 11.1492(17)$ Å, $c = 32.869(5)$ Å, $\beta = 98.807(2)$, $V = 5282.7(14)$ Å$^3$, $Z = 4$; $\rho_{calcd} = 1.844$ g cm$^{-3}$, $\mu(Mo_{K\alpha}) = 1.038$ mm$^{-1}$, $\theta_{max} = 27.48$, $T = 120$ K, 59356 total collected reflections, 12083 unique reflections, 1151 refined parameters, GOF = 1.138, $R_1 = 0.1360$ and $wR_2 = 0.2841$ for all data; $R_1 = 0.1018$ for 8764 independent reflections ($I > 2.0\sigma(I)$), min./max. electron density 2.787/−2.588 e Å$^{-3}$.

[13] Y. Matsunaga, Y. Maeda, T. Wakahara, T. Tsuchiya, M. O. Ishitsuka, T. Akasaka, N. Mizorogi, K. Kobayashi, S. Nagase, K. M. Kadish, *ITE Lett.* **2006**, *7*, 43 – 49.

[14] Y. Maeda, et al., *J. Am. Chem. Soc.* **2004**, *126*, 6858 – 6859.

[15] Compared with the traditional B3LYP functional, the M06 family of functionals has been shown to give more accurate geometries and energies for dispersion-dominated systems, such as benzene aggregates. Y. Zhao, D. G. Truhlar, *Theor. Chem. Acc.* **2008**, *120*, 215 – 241.

[16] M. J. Frisch et al., Gaussian 09, Revision A.02, Gaussian, Inc., Wallingford CT, **2009**.

[17] D. Kuciauskas, S. Lin, G. R. Seely, A. L. Moore, T. A. Moore, D. Gust, T. Drovetskaya, C. A. Reed, P. D. W. Boyd, *J. Phys. Chem.* **1996**, *100*, 15926 – 15932.

[18] C. Luo, D. M. Guldi, H. Imahori, K. Tamaki, Y. Sakata, *J. Am. Chem. Soc.* **2000**, *122*, 6535 – 6551.

[19] The energy level of the ion pair was evaluated using the Weller-type approach (see the Supporting Information). D. Rehm, A. Weller, *Isr. J. Chem.* **1970**, *7*, 259 – 271.

  